Effect of double injection on combustion, performance and emissions of Jatropha water emulsion fueled direct-injection diesel engine

Kim-Bao Nguyen

Dan, Tomohisa

Asano, Ichiro

(Citation)
Energy,80:746-755

(Issue Date)
2015-02-01

(Resource Type)
journal article

(Version)
Accepted Manuscript

(URL)
https://hdl.handle.net/20.500.14094/90003500

Effect of Double Injection on Combustion, Performance and Emissions of Jatropha Water Emulsion Fueled DI Diesel Engine

Kim-Bao NGUYEN[1], Tomohisa DAN[1,*], Ichiro ASANO[1]

[1] Faculty of Maritime Sciences, Kobe University

5-1-1 Fukaeminami, Higashinada-ku, Kobe, 658-0022, Japan

*Corresponding author:

Tomohisa DAN,

E-mail: dan@maritime.kobe-u-ac.jp

Phone: +81-78-431-6289

Address: 5-1-1 Fukaeminami, Higashinada-ku, Kobe, 658-0022, Japan.

Abstract

The experimental study was carried out using a four-stroke, high speed, direct-injection diesel engine with double fuel injections. In this study, Jatropha water emulsion was made by mixing a mass ratio of 10% of water. While fixing the first injection timing, we tested the engine on JWE with various injection timings and quantities of second injections. The acquired data was analyzed for various combustion parameters such as heat release rate, combustion center (timing of 50% of total heat release), ignition delay, and combustion duration; for performance parameters such as in-cylinder temperature, exhaust gas temperature, brake thermal efficiency; and emissions of CO, CO_2, HC, NOx, as well as dust and smoke opacity. When using a large second injection amount, we found a significant reduction in the peaks of the in-cylinder pressure, HRR, and average in-cylinder temperatures. We also found a drastic increase in the ignition delay, combustion duration, and a shift in the combustion center toward the later combustion stage, as well as increased exhaust gas temperatures, and reduced brake thermal efficiency compared with those of the Light oil. A large second injection amount reduced NOx emissions up to 48%, and drastically reduced HC emissions at higher loads of the engine.

Keywords: Jatropha oil, Jatropha water emulsion, Double fuel injection, Combustion, Emissions

1. Introduction

Diesel engines have been used widely in the transportation, construction work, and power generation due to their high thermal efficiency and durability. However, diesel engines have been faced with problems like the fossil fuel crisis, and the more stringent criteria regulated by governments attempting to protect the air quality. The main harmful pollutants, namely NOx (nitrogen oxides) and PM (particulate matters), which are trade-offs in using diesel engines, have been closely watched. Additionally, the production of global warming gas, CO_2 (carbon dioxide), is unavoidable whatever the fuel when using diesel engines. To allay these concerns, vegetable oils have recently gained attention as a promising alternative fuel for a greener future.

Short-term tests have revealed that most vegetable oils are capable of being used directly in existing diesel engines with little or no modification. However, long-term tests have reported some operational problems such as piston ring sticking, injector and engine deposits, gum formation and oil thickening [1]. This is primarily attributed to the high viscosity, poor volatility, and bulky molecules of the vegetable oils. These physical properties result in an increase in CO (carbon monoxide), HC (hydrocarbons) and PM, but lower NOx emissions compared to those of diesel oil alone [2-4]. Among vegetable oils, Jatropha has been of interest because it is not a food source [3].

Jatropha oil was identified as a leading candidate for an alternative fuel among various non-edible vegetable oils [5] since the plant does not suffer excessively from droughts, or needs not a concentrated irrigation, and therefore, unlike other common biofuel crops, the Jatropha plant can be cultivated easily even on poor and arid soil. The high viscosity, poor volatility, and low cetane number of Jatropha oil have been reported in the literature [6]. Higher smoke, HC, CO have been observed [3, 7, 8], while NOx emissions have also been reported lower when engines run on Jatropha oil [3, 8]. In the performance aspect, the brake thermal efficiencies of engines fueled with Jatropha oil have been generally lower in comparison with those using diesel oil [3, 6-9]. This is attributed to the physical-chemical-properties of Jatropha oil such as high viscosity, poor volatility, bulky molecular structure, and low cetane number. The drawbacks of Jatropha oil may be overcome by preheating [7, 8], and/or blending with diesel oil [10, 11], emulsification [12], or modifying injection strategy.

Advanced injection strategies are reported to be successful in reducing NOx emissions. The reduction of NOx is attributed to the cooling effect of the secondary injection [13]. Also it is attributed by the reduction of peak combustion pressure and peak heat release at the premixed combustion phase [14, 15], or the lower combustion temperatures and resident time of high temperatures [16]. The reduction of soot has been revealed in the literature [13-15, 17, 18] due to the reduction in precursor formation [13] and the reduction in particulate number concentration. Also it is because of the enhanced soot

oxidation by second injection [13, 15, 17] and the leaning-out spray and improved mixing with air [15, 18]. However, researches have also reported a reverse trend of higher NOx [17] and higher PM [19] with split injection.

The usage of water emulsion fuel is a well-known way to significantly reduce NOx emissions, and soot/PM from diesel engines as proven in the literature [20, 21-23]. The reduction of NOx is attributed to the cooling effect of the vaporization of water in the emulsion fuel [21-24]. While the reduction of soot is seen as a consequence of the better atomization and mixing with air resulting from micro-explosion [21, 23], or the presence of OH radicals releasing during the combustion process [21, 23], or more air entrainment [24]. A durability aspect of water emulsion, authors have examined a combustion state of Jatropha water emulsion fuel in a pre-combustion chamber type diesel engine. As the result, it was obtained that the water emulsion case can reduce drastically the carbon deposit on the nozzle surface [25]. Recently, Jatropha methyl ester emulsified with wood pyrolysis oil was tested and its benefit was observed [26].

From this one might surmise that a combination of an advanced injection strategy with Jatropha water emulsion may reduce both NOx emissions and soot in diesel engine. However, this combination has not been tried yet to the best of our knowledge. Our current experimental research was conducted to remedy this situation. We investigated the effect of double injection pattern and Jatropha water emulsion on the combustion, performance and emissions characteristics of a diesel engine. The double injections with various injection timings, and injection quantities of second injections were investigated in this study, while the first injections were fixed at the same timing.

2. Experimental setup and procedures

Experiments were conducted on a single cylinder, four-stroke, high speed, direct injection diesel engine (Yanmar Co., Ltd., Japan). The scheme of experimental setup is shown in Fig. 1a and the main specifications of the test engine are given in Table 1.

The mechanical fuel injection system of the engine was replaced by a common rail injection system, however, mechanical injector was remained. Main components of the common rail system include a motor-driven-pump (radial piston pump), a common rail (high pressure tube), an electronic injector, and an electronic control unit (ECU). The ECU was connected to a computer via a combustion analyzer (Yokogawa) to record the data. Injection parameters such as injection timing, injection duration, injection mode, along with rail pressure can be displayed on the ECU screen. Rail pressure can also be adjusted via the ECU, while, injection timing, and injection duration can be set through the ECU or the computer. The electronic injector of the common rail system is connected to the fuel tube of original mechanical injector. The fuel injected through

the electronic injector once accumulates in the fuel tube, and then it is injected into the combustion chamber through the mechanical injector.

The in-cylinder pressures were measured using a piezoelectric pressure transducer (Kistler) fitted into the cylinder of the engine and connected to a charge amplifier. The signals from the pressure transducer and the shaft encoder were acquired and transmitted to the computer via the combustion analyzer for recording the in-cylinder pressure and crank angle. Load of the engine was set through an electrical-dynamometer (Toyo Electric Co., Ltd.) coupled to the shaft of the engine. A set of gas analyzers VIA-510, CLA-510SS (Horiba) was used to measure the emissions of CO_2, NOx, respectively, and along with MEXA-324J (Horiba) for measurement of CO, HC. A smoke meter (Banzai) was used to measure the smoke opacity of the engine.

Dust matters were trapped on the paper filters (ADVANTEC PG-60, glass fiber Fluorine coated filter, Toyo Roshi Kaisha, Ltd.) in 10 liters of exhaust gas at each step of the experiments with the help of a gas sampler (D-25UP, OCT science, Ltd.). The gas sampler can be adjusted a flow rate and a volume of the exhaust gas flow through the sampler. The sampler will stop automatically when the volume of the gas going through the sampler reaches the setting value, 10 liters for this study. The paper filters were kept in a dust collector connecting to the exhaust pipe and the gas sampler. In each experiment step, we collected the dust on 4 paper filter sheets. The trapped paper filters were then dried at 50 ^{o}C in one hour to eliminate water content in the filters. They were averaged from the differences of the mass of the trapped filters and the mass original paper filters. These were dust. Afterward, SOF (soluble organic fraction) in the dust trapped filters was dissolved by dichloromethane and was calculated by balancing the mass of the filters before and after extraction (average value). ISF (in-soluble organic fraction) was calculated by subtraction of the paper filter mass after SOF dissolving and the original filter.

Measurements were carried out using LO (Light oil), JO (Jatropha oil) and JWE (Jatropha water emulsion) with a mixing rate of 10%. Prior of this study, the experiment of Jatropha emulsion with hydrogen peroxide was conducted [12]. In the experiments, Jatropha water emulsion tests were also carried out, and it was found that the 10% water mixing case gave the most stable engine operation. So, 10% water mixing rate was decided in this study. To make the emulsion fuel, a mixing system with a tank for JO; a tank for water; a circulating pump; and a static mixer was used. To keep the emulsion fuel homogeneous and stable, three kinds of surfactants (Rheodol SP-L 10, Rheodol 440V, and Emulgen 103, Kao Chemicals Corp., Japan) were used. Specifications of the surfactants are given in Table 2. A schematic diagram of the mixing system is shown in Fig. 1b.

The engine was fed with LO, and JO with single injection at the injection timing set by the engine maker of -17 deg. CA. ATDC for baseline data. To investigate the effect of injection pattern and the JWE, the first injection was kept at -23 deg. CA ATDC and the second injection was set at 0, +3, +6 deg. ATDC for double injection mode. After a preliminary investigation for the lowest smoke opacity, the optimum timing of second injection was chosen to conduct experiments for measurement of dust, SOF and ISF with different injection quantities in the second injection (hereafter called small and large). The operational conditions (injection quantities) of the experiments are provided in Table 3. The mass of Jatropha and water was weighed to create emulsion fuel prior to the experiments with a 10% mixing ratio of water. While, the Jatropha oil was circulating from the tank through the pump, the water was supplied from the water tank through a needle valve which was used to control mixing rate for a homogeneous mixture of emulsion fuel. Table 4 provides the properties of the test fuels. The fatty acid compositions of the Jatropha oil are given in Table 5.

All experimental steps were conducted at room temperature and the results were recorded at steady operational conditions of the engine. During the experiments, the engine load was set at different values of 3.0 kW, 4.5 kW, and 6.0 kW with a speed of 2000 rpm, while the rail pressure was kept at 100 MPa. The gas emissions including CO, CO_2, HC, smoke, and NOx were measured during each step of the experiments.

3. Results and discussions

3.1 Combustion characteristics

The combustion process of a diesel engine depends on the fuel-air mixing process and is related to fuel properties, such as viscosity, volatility. And the fuel injection system itself also affects to the combustion process. With a common rail diesel engine, the operational parameters in terms of injection mode including the number of injections, injection timing, and quantity of injections strongly affect the combustion process. In this section, the combustion characteristics are demonstrated by number of factors, namely combustion pressure, heat release rate, ignition delay, combustion duration, and center of combustion.

In-cylinder pressure of the engine is indicated in Fig. 2. It is clear that the peak pressures of the engine depend on the injection pattern as well as the fuel. The peaks of pressures were lower for the JO fueled engine in comparison with those of the LO. This is because of the lower heating value of the JO fuel, its lower volatility, and the higher viscosity of the JO. For the injection patterns of JWE-23/0 and JWE-23/+3-large, the peak pressures were lower than those of the LO and JO. This resulted from less fuel in first injection of these double injection patterns when compared with JO. Moreover, the cooling

effect of the water in the emulsion fuel could reduce the combustion rate and pressure development. While, the peak pressures of JWE-23/+3-small and JWE-23/+6 were higher than those of LO. In these injection patterns, the larger amount of fuel in the first injection, and the timing of the second injection was far away the TDC, respectively, thus the second injection combusted immediately after fuel injection. Consequently, the in-cylinder pressure's intensity was the highest. The combustion of double injection patterns started earlier than for single injections of LO, and JO as a result of earlier injection timing of the first injection when compared to the injection timing of the single injection mode.

Heat release rate (HRR) in the cylinder of the engine is presented in Fig. 3. The sharpest and highest increments of HRR were seen for the LO. The peaks of the HRR were 63, 58, and 53 J/deg. for 3.0, 4.5, and 6.0 kW, respectively. The fast combustion of the LO results from the physical properties of fossil fuel, such as low viscosity, and high volatility, thus it is easier to atomize and mix with air. The maximum of the HRR was lower for the JO and emulsion fuel in most injection patterns. The peaks of the HRR were around 49 J/deg. for the JO. This is equivalent to relative reductions of 22, 15.8, and 7.2 % when compared with those of the LO. This is due to the lower heating value and lower combustion rate of vegetable oil as a result of its physical properties. The injection patterns of JWE-23/+3-small and JWE-23/+6 significantly reduced HRR; while, the HRR dropped suddenly with the injection patterns of JWE-23/+3-large and JWE-20/0. The former generated relative reductions of 48, 25% and 34, 27% when the peaks of HRR reduced to 43 J/deg. or 33 J/deg. for 3.0, and 4.5 kW, respectively. The later showed maximum reduction of 75, 56, 46% and 71, 63, 44% when peaks of HRR dropped to 16, 25, 28 J/deg., and 18, 21, 30 J/deg. for 3.0, 4.5, and 6.0 kW, respectively. This resulted from the reduction in the concentration of fuel spray as a result of split injection. Moreover, the cooling effect of the water content in the emulsion fuel was also a reason for reduction of the HRR. The earlier HRR for JWE fuel was a consequence of the earlier injection timing of the first injection when compared to those of the LO and JO.

The center of combustion, at which 50% of total heat release occurs, is indicated in Fig. 4a. It can be seen that the center of combustion shifted to the later stage when the JWE and double injection were utilized. For the LO, the combustion center was at 14.8 to 17.8 deg. ATDC. For the JO, a relative increment of timing of combustion center was 7.3% to 10% for 3.0 to 6.0 kW. While, for JWE-23/0 and JWE-23/+3-large the centers of combustion were at 21.5 to 29 deg. ATDC with relative increments of 46% to 63% when compared with those of the LO. For the JWE-23/+3-small and JWE-23/+6, the combustion center was at 16 to 20 deg. ATDC, with a relative increment of 11% to 20% in comparison with those of the LO. The later combustion center of biofuel is due to the lower rate of combustion, and later timing of second injection with double injection pattern.

Ignition delay is shown in Fig. 4b. The ignition delay is the duration from the start of injection to the start of combustion. The start of combustion is determined by the timing at which the HRR changes from a negative to a positive value. The ignition delay was shorter with an increase in the power of the engine as a consequence of the better combustion conditions such as temperature and pressure inside the combustion chamber. The ignition delays of the engine using the JWE fuel in double injection patterns were longer than those of the LO with relative increments of 48% to 59% when IDs were around 1.76 msec. to 1.60 msec. Longer ignition delay of JWE resulted from the cooling effect and the dilution of the water content in the JWE fuel. Moreover, for double injection patterns, at the start of injection, the pressures and temperatures inside the combustion chamber were lower than those of the LO and JO will results in increasing the ID. Slight reductions in the ID with different patterns were due to difference in the first injection quantities.

Combustion duration is indicated in Fig. 4c. Combustion duration is calculated from the start of combustion to the end of combustion (EOC). The EOC is determined by the timing of 95% total heat release. It can be seen that the CDs of the JWE with double injection were longer than those of the LO, and JO with single injection. The EOCs were at 50, 60, and 70 deg. ATDC for the LO fuel. While, for JWE-23/+3-small and JWE-23/+6, they were at 64 to 77 deg. ATDC. But, they were at 65 to 99 deg. ATDC and at 71 to 94 deg. ATDC for the injection patterns of JWE-23/0, and JWE-23/+3-large. This resulted from the larger amount of fuel in the second injection. Less fuel in the second injection and more fuel in the first injection for the JWE-23/+3-small and JWE-23/+6 resulted in shorter CDs when compared with those of the other injection patterns.

3.2 Performance characteristics

The performance parameters of the engine, such as in-cylinder and exhaust gas temperatures, and brake thermal efficiency are introduced in this section. In-cylinder temperature was calculated from the in-cylinder pressure history. Exhaust gas temperature was measured by a thermocouple and recorded during the experiments. Brake thermal efficiency was calculated as the ratio of the brake power to the energy supplied by the fuel consumption.

Average in-cylinder temperature is presented in Fig. 5. It can be seen that most double injection patterns showed lower peaks in in-cylinder temperatures when compared with those of LO. The reduction in in-cylinder temperatures are attributed to the cooling effect of the water content in the emulsion fuel, the reduction of fuel injected in the first injection when compared with single injection mode for the LO and JO. At 3.0 kW, the in-cylinder temperature increased from 1192 K with LO to 1199 K when the injection pattern of JWE-23/+6 with only a minor relative increment of 0.6%. Earlier and faster development of in-cylinder temperatures with large amount of fuel in the first injection for patterns of JWE-23/+3-small

and JWE-23/+6 were shown. But, in-cylinder temperatures developed later and the peaks of the in-cylinder temperatures were lower for the JWE-23/+3-large and JWE-23/0. In these injection patterns, at 3.0, 4.5, 6.0 kW, the peaks of the in-cylinder temperatures reduced from 1192, 1350, and 1518 K for the LO to 1140, 1265, and 1387 K for the JWE-23/0; and to 1123, 1245, and 1422 K for the JWE-23/+3-large, respectively. One can also see that the double injection increased temperature at a later stage, particularly, for JWE-23/+3-large and JWE-23/0. The value and timing of the peak in-cylinder temperatures have a great influence on NOx emissions.

Exhaust gas temperature is shown in Fig. 6a. Exhaust gas temperatures increased with increase in the engine power. This is due to the increased fuel injected and combustion which generates more engine power. When compared with the LO, the exhaust gas temperatures of the double injection increased much more with the injection patterns of JWE-23/0 and JWE-23/+3-large. However, for the JWE-23/+3-small and JWE-23/+6, only slight increments in the exhaust gas temperatures were found in comparison with those of LO. The exhaust gas temperatures increased from 292, 375, 481 ^{o}C for the LO to 389, 460, 607 ^{o}C for the JWE-23/+3-large; and to 305, 388, 493 ^{o}C for the JWE-23/+3-small, at 3.0, 4.5, and 6.0 kW, respectively. These are equivalent to relative increments of 16, 23, and 26%; and 4.5, 3.6, and 2.5%, respectively. Differences in injection patterns have different first injection mass which may explain these results. For the JWE-23/0 and JWE-23/+3-large, large amount of injected fuel in the second injection shifted the combustion to a later stage, and as a result, it increased the exhaust gas temperatures. This is consistent with the results of in-cylinder temperatures as shown previously. The minor increments in the exhaust gas temperatures for the JWE-23/+3-small and JWE-23/+6 when compared with those of the LO are attributed to the double injection pattern with less injected fuel in the second injection. The in-cylinder temperature, and exhaust gas temperature are strongly related to the brake thermal efficiency of the engine.

Specific fuel consumption (SFC) of the engine is displayed in Fig. 6b. These results were achieved after eliminating the water content for the emulsion fuel. The lowest SFC was for the LO due to the best combustion properties of the LO fuel. It decreased with an increase of the engine power. This is because the better combustion conditions at the higher engine powers. When compared with those of the JO, most emulsion fuel with double injections increased the SFC except the JWE-23/+3-small. At the higher powers, the lowest SFC of 348 and 338.2 g/kWh were achieved by the JWE-23/+3-small at 4.5 and 6.0 kW, respectively. This is resulted from the combustion characteristics as shown previously.

Brake thermal efficiency (BTE) of the engine is indicated in Fig. 6c. It is clear that the highest BTE was achieved by using LO. The single injection with JO, and double injection with JWE had lower BTE. This resulted from the combustion

characteristics of the biofuel as explained above due to the physical properties of the biofuel itself. Increased ignition delay, later combustion center, and longer combustion duration are reasons for reduction of the BTE, particularly, for the JWE-23/0 and JWE-23/+3-large. At 3.0, 4.5, and 6.0 kW, BTE were 30.5, 33.4, and 33.9% for the LO; and were 22.5, 25.7, and 26.7% for the JO. While, they were 21.9, 24.1, and 25% for the JWE-23/+3-large; and were 22.5, 26.0, 26.8 % for the JWE-23/+3-small. It is clear that the BTE increased with an increase in first injection quantity seen in the injection patterns of JWE-23/+3-small or JWE-23/+6. Moreover, for the JWE-23/+3-small, the BTE were comparable to those of the JO.

3.3 Emissions characteristics

The emissions of the engine including gas emissions such as CO_2, CO, HC, and NOx are indicated in Fig. 7. The smoke opacity, dust, soluble organic fraction, and in-soluble organic fraction are shown in Fig. 8.

Emission of CO_2 is presented in Fig. 7a. It is clear that the emissions of CO_2 were higher for biofuel including JO and JWE when compared with LO. Combustion of biofuel lasted to later phase due to slower combustion characteristics and double injections, therefore, the engine consumed more fuel to generate the same power thus increased emission of CO_2. It is also clear that different injection patterns made differences in the emissions of CO_2. The JWE-23/0 and JWE-23/+3-large induced the highest increments of CO_2, while the JWE-23/+3-small and JWE-23/+6 gave less increments of CO_2. For the JWE-23/0, relative increments of CO_2 were 16 to 21.5%, while they were 30.5 to 40% for the JWE-23/+3-large when compared with those of the LO. However, the JWE-23/+3-small and JWE-23/+6 had relative increments of 7.8% to 14% when compared with CO_2 emissions with the LO. This resulted from more injected fuel in the second injection in the injection patterns of JWE-23/0 and JWE-23/+3-large, and vice versa in the injection patterns of JWE-23/+3-small and JWE-23/+6. This is also relevant to the combustion characteristics as explained previously.

Emission of CO is shown in Fig. 7b. This figure shows clearly that the emissions of CO of biofuel were much higher than those of the LO, especially, for the JWE fuel. At 3.0, 4.5, 6.0 kW, the emissions of CO of the JWE-23/+3-large had 2.4 and 17.3 times higher than those of the LO, while for the JWE-23/+6, they were 1.1, 19.8 and 3.5 times higher than the LO. But, for the JWE-23/+3-small, the emissions of CO were 1.7, 7.4, 3.6 times higher than those of the LO at 3.0, 4.5, and 6.0 kW. Very high increments of the CO when using the JWE-23/+3-large and JWE-23/+6 at 4.5 kW are probably attributed to the cooling effect of the water content in the JWE and the late timing of the second injection. At 6.0 kW, in these injection patterns, the emissions of CO were reduced when compared with those at 4.5 kW. This is probably due to the dominant effect of higher in-cylinder temperatures, so there was less effect of cooling. The higher the combustion temperature, the

better the second atomization as a result of micro-explosion of water droplets in the emulsion fuel. And the more CO converted to CO_2. Finally, it reduced emissions of CO in comparison with those at 4.5 kW. For the JWE-23/+3-small, emission of CO was kept almost constant at 3.0 and 4.5 kW, it comparably increased to that of the JWE-23/+6 at 6.0 kW. To achieve higher engine power, a rich injection occurred where much more fuel was injected into the combustion chamber and this increased the amount of CO.

HC emission is indicated in Fig. 7c. The emission of HC depends on the power of the engine, the injection pattern, and the fuel. The emissions of HC decreased with an increase in the engine power. This is due to the higher combustion temperatures at higher engine powers. The biofuels produced much higher HC emissions especially at low loads. At 3.0 kW, the maximum increment of HC was 113% for the JWE-23/+3-large, while it was a minimum of 86% for the JWE-23/+3-small when compared with those of LO. At low engine power, with low combustion temperatures, the cooling effect of a large amount of fuel injected in the second injection for the JWE-23/+3-large increased the emissions of HC much more than for the 23/+3-small. At higher engine powers, the emissions of HC of the JWE were higher than those of the LO, but they were lower than those of JO when the JWE-23/0 and JWE-23/+3-large were used. In these injection patterns, less fuel injected in the first injection, along with probably micro-explosions at higher combustion temperatures, the dilution and better mixing of the fuel and air in the combustion chamber reduced emissions of HC when compared with those of JO. In the injection patterns of the JWE-23/+3-small and JWE-23/+6, the first injection quantity was large, thus an over rich mixture was generated, and the cooling effect dominated over the effect of micro-explosion. Then the amount of HC was higher than that of the JO.

Fig. 7d displays NOx emissions of the engine. The emissions of NOx had a strong correlation to the fuel and injection patterns. It is clear that combustion of the LO released more NOx than the biofuels. This is due to its higher heating value and higher combustion rate than the biofuels. We found a slight reduction of the NOx when using the injection patterns of JWE-23/+3-small and JWE-23/+6 for the JWE fuel, while, a significant reduction of NOx emissions was found for injection patterns of the JWE-23/0 and JWE-23/+3-large. Maximum reductions of NOx in these injection patterns were 45 to 54% when compared with those of the LO. This is a consequence of the combustion characteristics as explained previously. The HRR in these injection patterns dropped suddenly because less fuel was injected. It reduced the maximum temperatures in the combustion spots of the fuel spray, which result in reducing of the NOx emissions. The marginal reduction of NOx emissions for the JWE-23/+3-small and JWE-23/+6 is attributed to the increased first injection quantity leading to less reduction in the HRR.

Smoke opacity is indicated in Fig. 8a. The smoke emission was measured to find the optimum injection timing of the second injection before measuring dust, ISF, and SOF. We measured smoke when running the engine on JWE, and double injection pattern with a fixed first injection timing, and various second injection timings of 0, +3, +6 deg. ATDC. Fig. 8a shows that smoke opacity was comparable at 3.0 kW, and it increased with increase in engine power. This is because more fuel was injected into the combustion chamber for the higher loads. Moreover, the different injection timings of the second injection indicated different smoke opacities. Higher smoke opacities were found with early or late timing of the second injection. This resulted from the cooling effect of the large amount of fuel in the second injection at the TDC. The rich mixture in the first injection and reduced-combustion temperatures were occurred when the second injection started for the late injection. The optimum injection pattern was JWE-23/+3 for lower smoke emissions.

Concentration of ISF, SOF, and dust are displayed in Fig. 8b-d. These show that the dust emissions were higher for biofuels at lower loads of the engine in comparison with those of the LO. At 3.0 kW, the concentrations of dust was comparable at around of 0.26 g/m^3, while it was 0.09 g/m^3 for the LO. The higher viscosity of the biofuels and the cooling effect of the emulsion fuels increased the ISF and SOF, and thus consequently increased the dust concentrations. At higher engine powers, the fastest developments of dust concentrations were for the JEW-23/+3-large with relative increments of 2.3 and 0.6 times when compared with those of the LO. Large amount of the second fuel injection under high burning gas temperatures enhanced the conversion of fuel into the ISF, while reduced the SOF. The JWE-23/+3-small with more first injection quantity and longer time for the oxidation process reduced the ISF. We found less increment of the dust concentration in this injection pattern. At 6.0kW, the lower dust concentration of the JO in comparison with those of the LO is attributed to the higher oxygen content in the vegetable oil that probably reduced the ISF as shown in this figure.

4. Conclusions

A direct injection diesel engine operated with Jatropha water emulsion was used to investigate the effects of double injection patterns and JWE fuel on the combustion, performance and emissions of the engine. In summary, the main features are as follows.

1- Large amount of fuel in the second injection in injection patterns such as JWE-23/0 and JWE-23/+3-large drastically reduced the peaks of in-cylinder pressure and the peak of HRR. Also it increased significantly the ignition delay, combustion duration, and shifted the combustion center toward the later stage. For small amount of fuel in the second

injection such as JWE-23/+3-small and JWE-23/+6, the peaks of the in-cylinder pressures were higher, while, other parameters had the same tendency with lower intensity when compared with those of the LO.

2- Large amount of fuel in the second injection drastically reduced the in-cylinder temperatures, increased the exhaust gas temperatures, and lowered the BTE in comparison with those of the JO. The opposite occurred when small second injection amount was used as in JWE-23/+3-small and JWE-23/+6. We also found that when using the JWE-23/+3-small the BTE was higher than that of the JO.

3- The emulsion fuel and double injection increased CO_2, CO, and HC emissions when compared with those of the LO. However, in comparison with those of the JO, the large second injection quantity such as the JWE-23/+3-large reduced the HC emissions. NOx emissions were related to the combustion characteristics of the engine with different injection patterns. The emulsion fuel, and double injection patterns reduced NOx emissions when compared with those of the LO. Large second injection amount such as the JWE-23/0 and JWE-23/+3-large significantly reduced the NOx emissions.

4- In three timing tests, the JWE-26/+3 reduced smoke opacity when using JWE and double injection. The ISF was the main element, while the SOF was a minor element of the dust. Large second injection amount increased the ISF and dust concentration much more than a small second injection amount.

Acknowledgement

We would like to acknowledge our Lab-members, Mr. HISASIBA, Mr. MATSUMOTO, Mr. TANAKA and Mr. YOSHIDA, at the Internal Combustion Engineering Laboratory, Faculty of Maritime Sciences, Kobe University for their help in conducting the experiments.

References

[1] R. Altın, S. Çetinkaya and H. S. Yücesu. The potential of using vegetable oil fuels as fuel for diesel engines. Energy Conversion and Management 2001, Volume 42, p. 529-538.

[2] N. Hemmerlein, V. Korte, H. Richter and G. Schröder. Performance, exhaust emissions and durability of modern diesel engines running on rapeseed oil. SAE Technical Paper 910848, 1991.

[3] M. S. Kumar, A. Ramesh, B. Nagalingam. An experimental comparison of methods to use methanol and Jatropha oil in a compression ignition engine. Biomass and Bioenergy 2003, Volume 25, p. 309-318.

[4] A.S. Huzayyin, A.H. Bawady, M.A. Rady, A. Dawood. Experimental evaluation of diesel engine performance and emission using blends of jojoba oil and diesel fuel. Energy Conversion and Management 2004, Volume 45, p.2093-2112.

[5] S.-Y. No. Inedible vegetable oils and their derivatives for alternative diesel fuels in CI engines: A review. Renewable and Sustainable Energy Reviews 2011, Volume 15, p.131-149.

[6] K. Pramanik. Properties and use of jatropha curcas oil and diesel fuel blends in compression ignition engine. Renewable Energy 2003, Volume 28, p. 239-248.

[7] Deepak Agarwal, Avinash Kumar Agarwal. Performance and emissions characteristics of Jatropha oil (preheated and blends) in a direct injection compression ignition engine. Applied Thermal Engineering 2007, Volume 27, p. 2314-2323.

[8] B. S. Chauhan, N. Kumar, Y. D. Jun, K. B. Lee. Per**for**mance and emission study of preheated Jatropha oil on medium capacity diesel engine. Energy 2010, Volume 35, p. 2484-2492.

[9] A. K. Agarwal and A. Dhar. Performance, emission and combustion characteristics of preheated and blended Jatropha oil. Chapter 26 in "Jatropha, Challenges for a New Energy Crop", Volume 1: Farming, Economics and Biofuel by Carels, Nicolas, Sujatha, Mulpuri, Bahadur, Bir (Eds.).

[10] B. S. Chauhan, N. Kumar, H. M. Cho. A study on the performance and emission of a diesel engine fueled with Jatropha biodiesel oil and its blends. Energy 2012, Volume 37, p. 616-622.

[11] M. Mofijur, H. H. Masjuki, M. A. Kalam, A. E. Atabani. Evaluation of biodiesel blending, engine performance and emissions characteristics of Jatropha curcas methyl ester: Malaysian perspective. Energy 2013, Volume 55, p. 879-887.

[12] K-B. Nguyen, T. Dan. I. Asano. Combustion, Performance and Emission Characteristics of Direct Injection Diesel Engine Fueled by Jatropha Hydrogen Peroxide Emulsion. Energy 2014, Volume 74, pp.301-308.

[13] L. D. K. Nguyen, N. W. Sung, S. S. Lee, and H. S. Kim. Effect of split injection, oxygen enriched air and heavy EGR on soot emissions in a diesel engine. International Journal of Automotive Technology 2011, Volume 12, p. 339-350.

[14] M. Y. Kim, S. H. Yoon, and C. S. Lee. Impact of split injection strategy on the exhaust emissions and soot particulates from a compression ignition engine fueled with neat biodiesel. Energy & Fuel 2008, Volume 22, p. 1260-1265.

[15] R. Mobasheri, Z. Peng, S. M. Mirsalim. Analysis the effect of advanced injection strategies on engine performance and pollutant emissions in a heavy duty DI-diesel engine by CFD modeling. International Journal of Heat and Fluid Flow 2012, Volume 33, p. 59-69.

[16] D. Qi , M. Leick, Y. Liu, C. F. Lee. Effect of EGR and injection timing on combustion and emission characteristics of split injection strategy DI-diesel engine fueled with biodiesel. Fuel 2011, Volume 90, p.1884-1891.

[17] S. H. Park, S. H. Yoon, C. S. Lee. Effect of multiple-injection strategies of overall spray behavior, combustion and emissions reduction characteristics of biodiesel fuel. Applied Energy 2011, Volume 88, p. 88-98.

[18] C.Y. Choi, R.D. Reitz. An experimental study on the effects of oxygenated fuel blends and multiple injection strategies on DI diesel engine emissions. Fuel 1999, Volume 78, p.1303-1317.

[19] K. Yehliu, A. L. Boehman, O. Armas. Emissions from different alternative diesel fuels operating with single and split fuel injection. Fuel 2010, Volume 89, p. 423-437.

[20] R. J. Crookes, F. Kiannejad, and M. A. A. Nazha. Systematic assessment of combustion characteristics of biofuel and emulsions with water for use and diesel engine fuels. Energy Conversion and Management 1997, Volume 38, p. 1785-1795.

[21] O. Armas, R. Ballesteros, F. J. Martos, J. R. Agudelo. Characterization of light duty diesel engine pollutant emissions using water-emulsified fuel. Fuel 2005, Volume 84, p. 1011-1018.

[22] J. Ghojel, D. Honnery, K. Al-Khaleefi. Performance, emissions and heat release characteristics of direct injection diesel engine operating on diesel oil emulsion. Applied Thermal Engineering 2006, Volume 26, p. 2132-2141.

[23] R. Ochoterena, A. Lif, M. Nyden, S. Andersson, I. Denbratt. Optical studies of spray development and combustion of water-in-diesel emulsion and microemulsion fuels. Fuel 2010, Volume 89, p. 122-132.

[24] A. Maiboom, X. Tauzia. NOx and PM emissions reduction on an automotive HSDI diesel engine with water-in-diesel emulsion and EGR: An experimental study. Fuel 2011, Volume 90, p. 3179-3192.

[25] N. Miyawaki, T. Dan, M. Hashimoto, I. Asano. Improvement of combustion characteristics of Jatropha oil by water emulsification – Combustion analysis in pre-combustion chamber type diesel engine. Journal of the Japan Institute of Marine Engineering 2011, Volume 46 No.5, p.752-757.

[26] R. Prakash, R.K. Singh, S. Murugan. Experimental investigation on a diesel engine fueled with bio-oil derived from waste wood-biodiesel emulsions. Energy 2013, Volume 55, p. 610-618.

LIST OF FIGURES

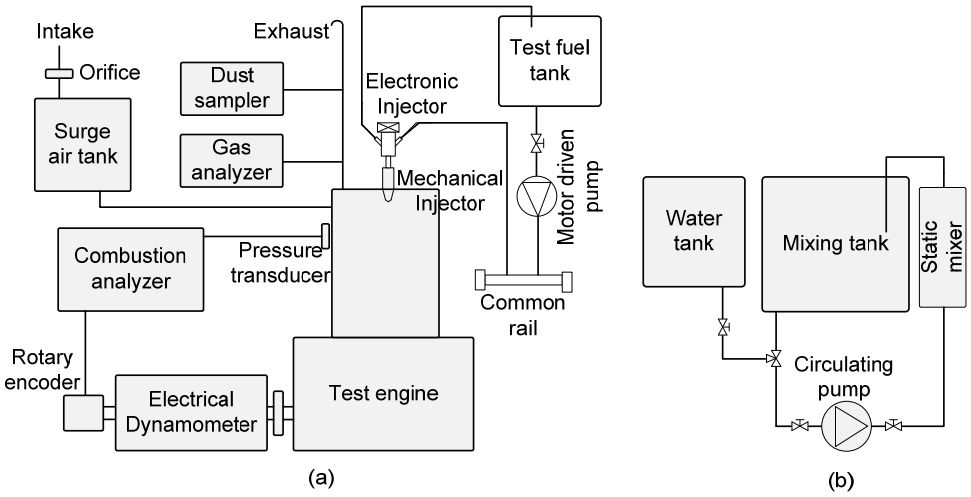

Figure 1 Schematic diagram of (a) experimental set-up, and (b) mixing system

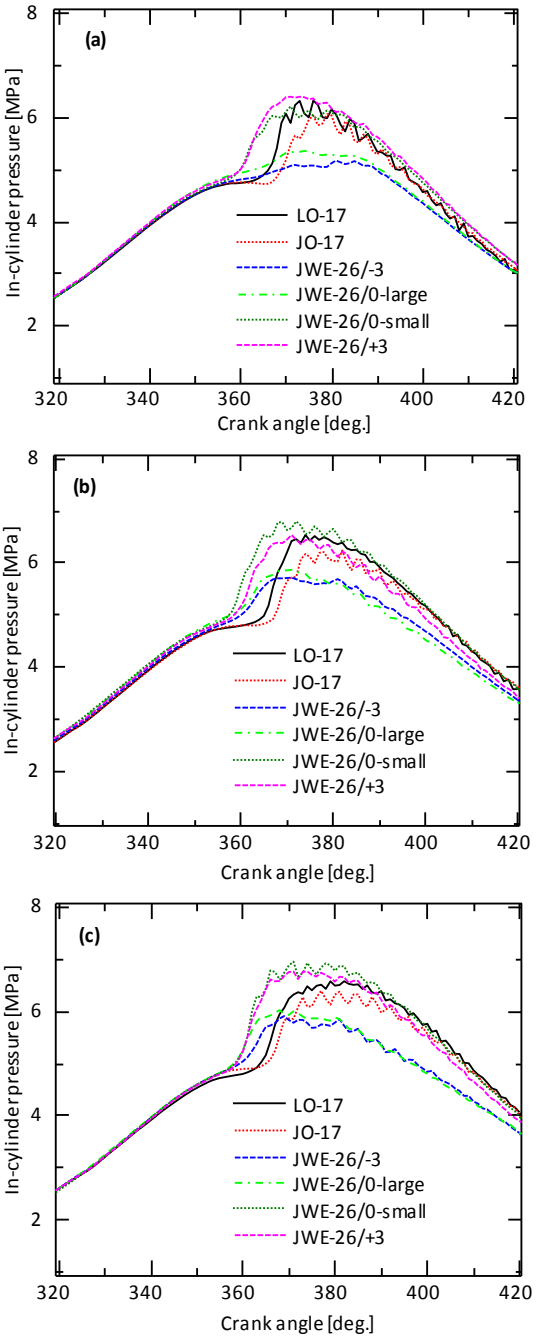

Figure 2 In-cylinder pressures at engine power of (a) 3.0 kW, (b) 4.5 kW, and (c) 6.0 kW at a constant speed of 2000 rpm

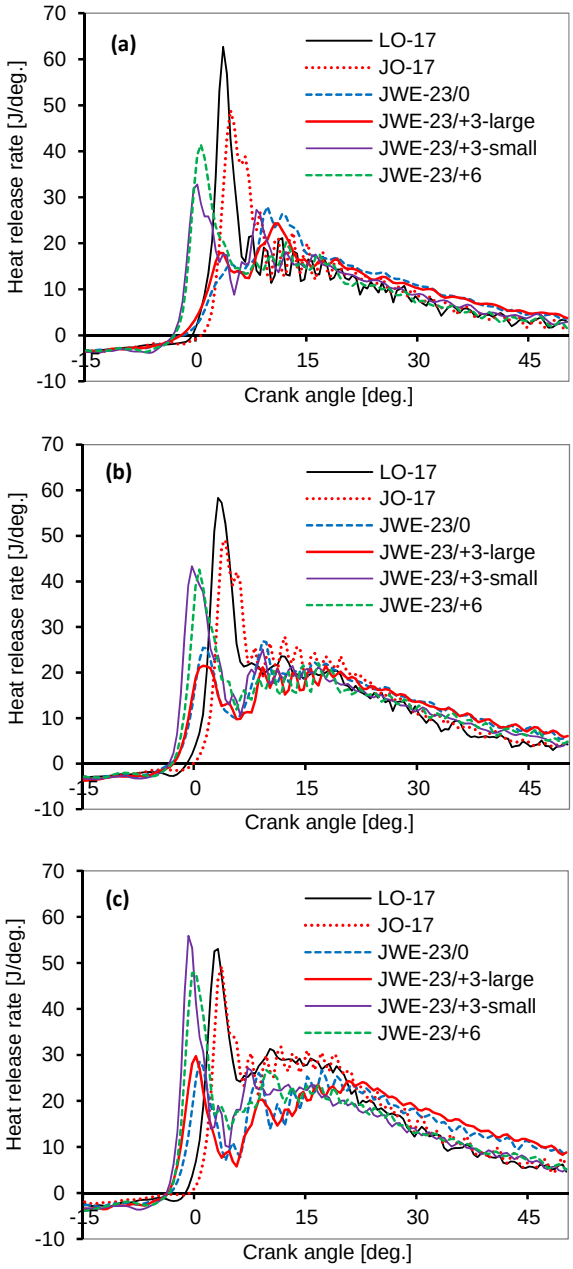

Figure 3 Heat release rate at engine power of (a) 3.0 kW, (b) 4.5 kW, and (c) 6.0 kW at a constant speed of 2000 rpm

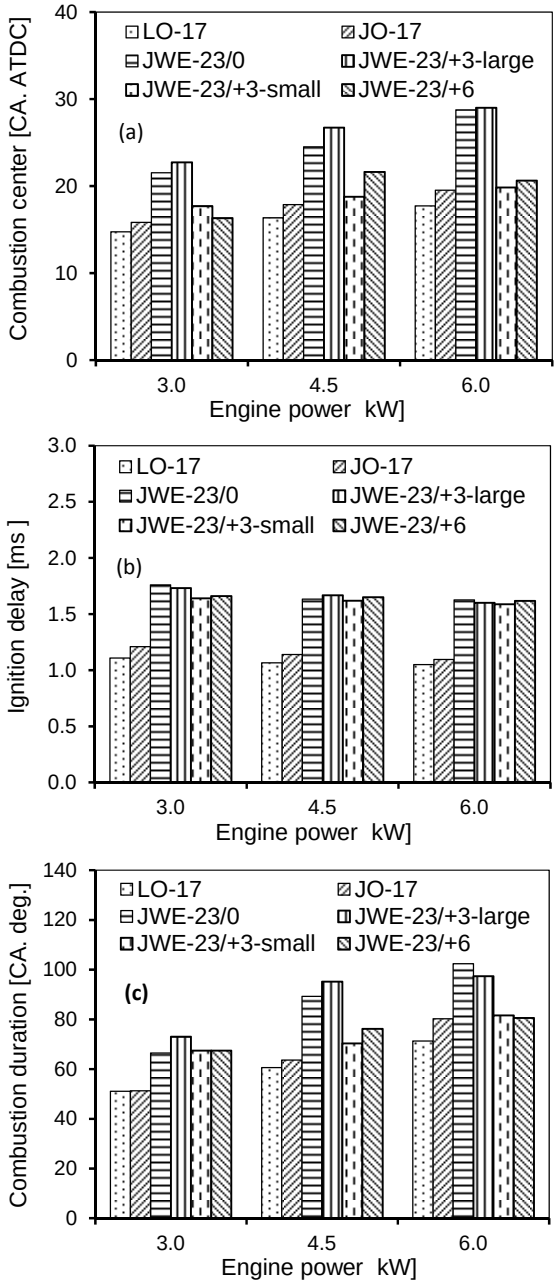

Figure 4 (a) Combustion center, (b) ignition delay, and (c) combustion duration of the engine at a constant speed of 2000 rpm

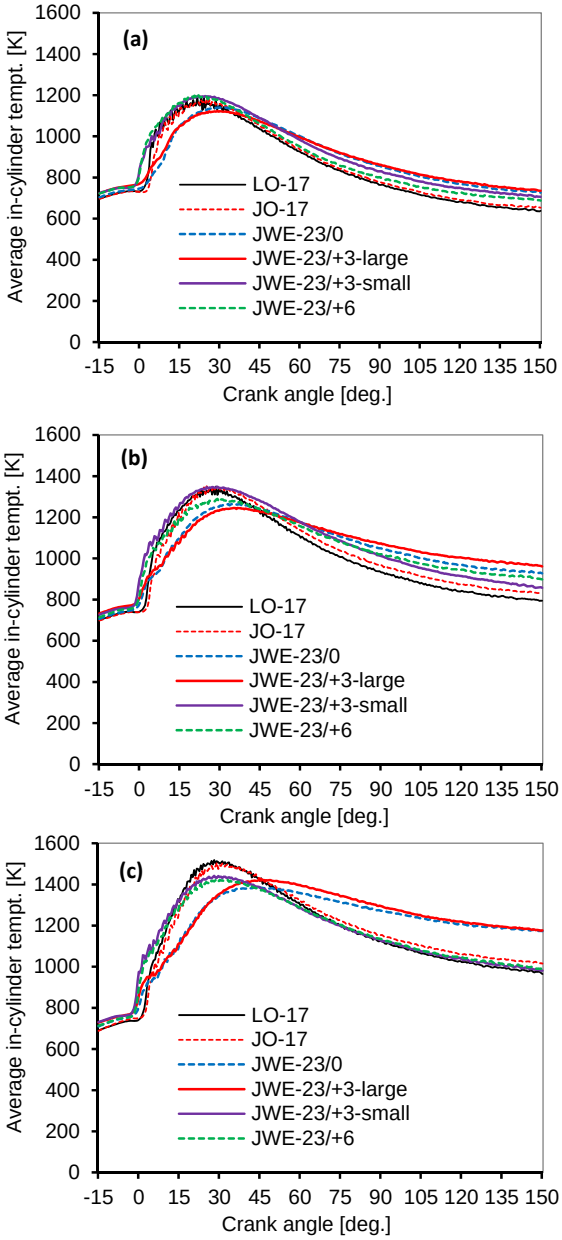

Figure 5 Average in-cylinder temperatures at engine power of (a) 3.0 kW, (b) 4.5 kW, and (c) 6.0 kW at a constant speed of 2000 rpm

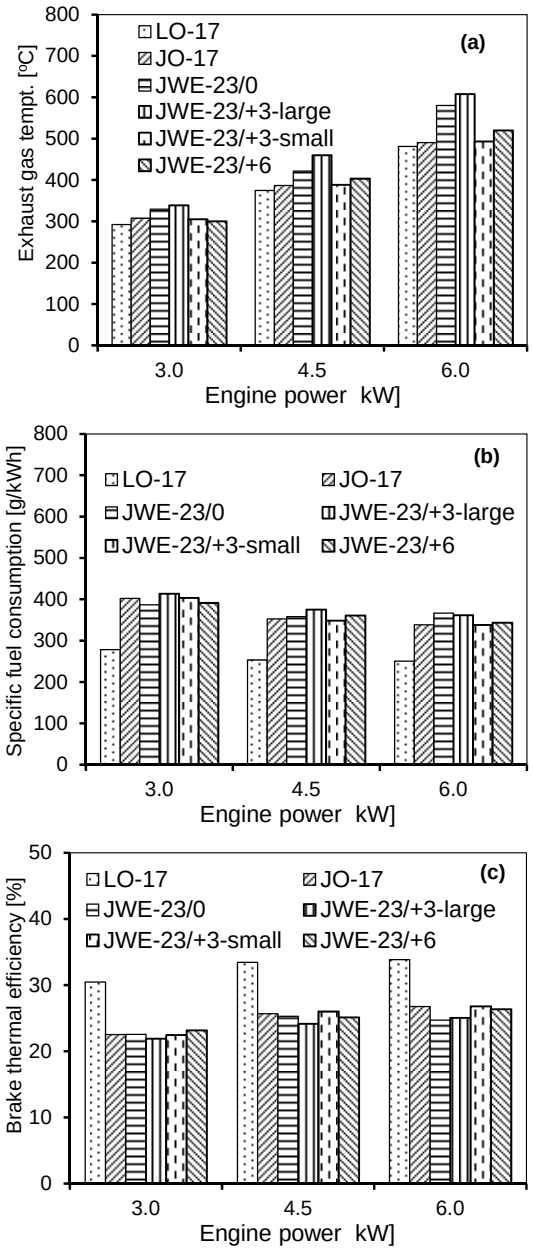

Figure 6 (a) Exhaust gas temperatures, (b) specific fuel consumption, and (c) brake thermal efficiency of the engine at a constant speed of 2000 rpm

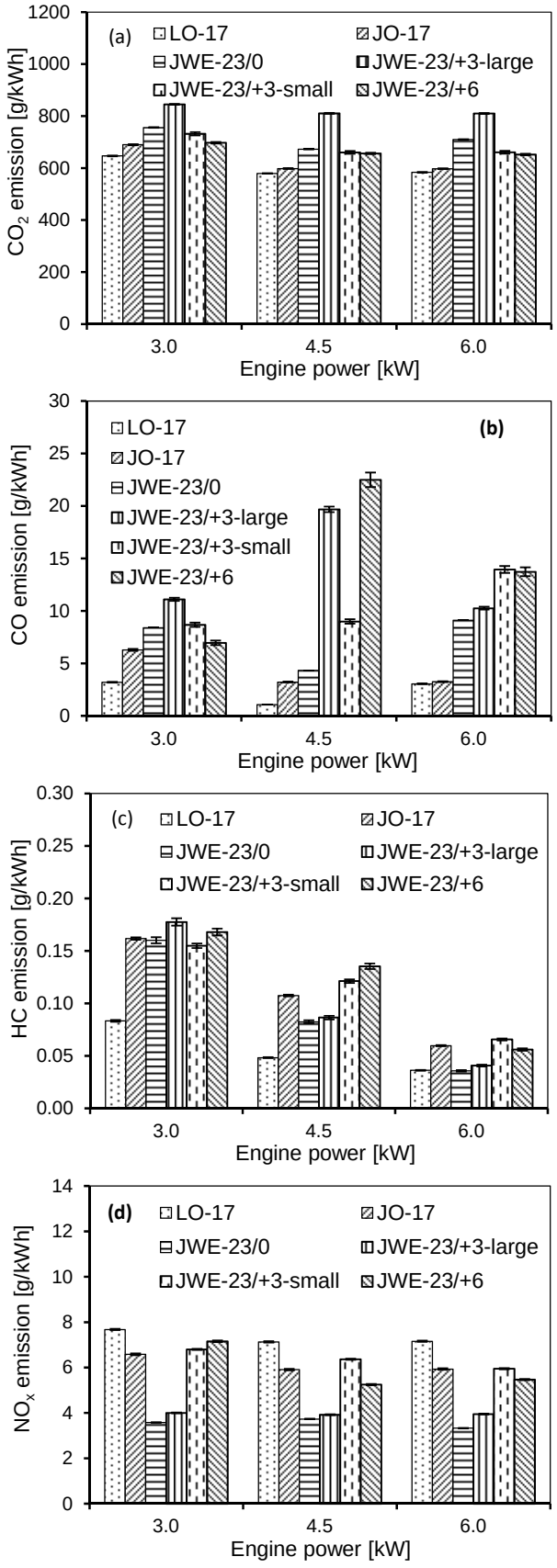

Figure 7 Exhaust gas emissions of the engine at a constant speed of 2000 rpm

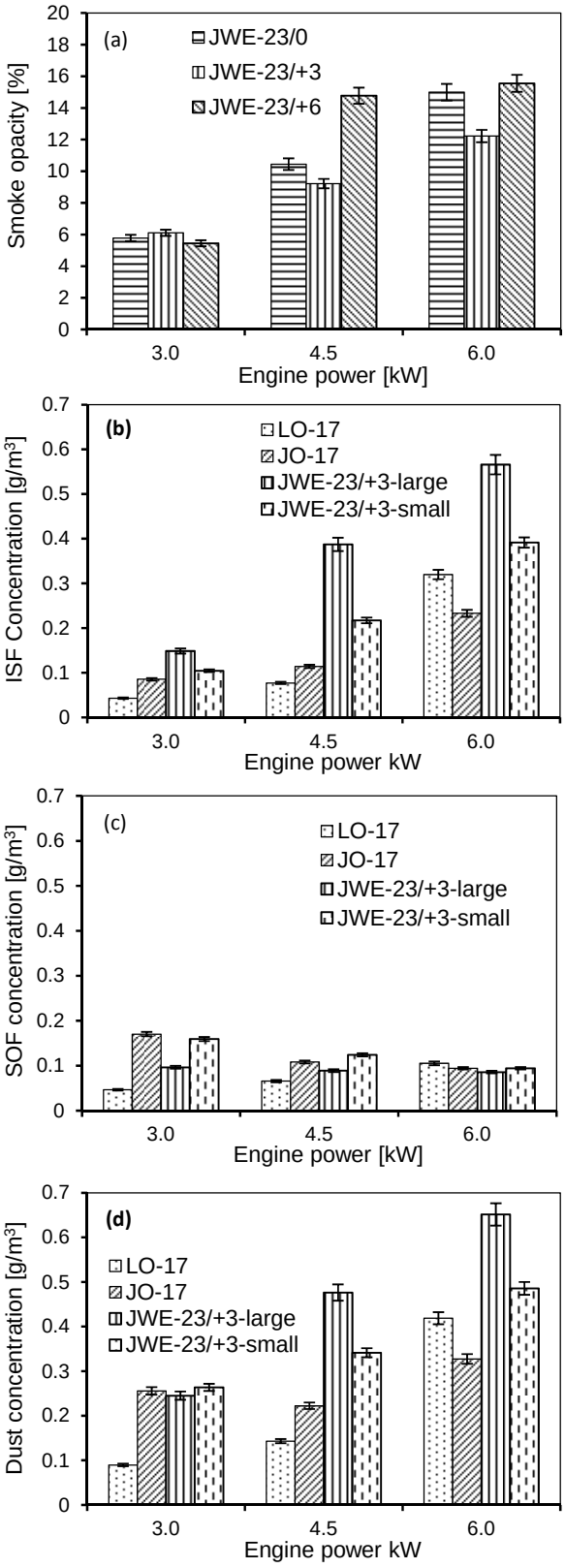

Figure 8 (a) Smoke opacity; (b) ISF, (c) SOF, and (d) dust concentration of the engine at a constant speed of 2000 rpm

LIST OF TABLES

Table 1 Specifications of test engine

	Specification
Model	YANMAR NFD 13-ME
Engine type	Horizontal, 1-cylinder, 4-stroke
Combustion type	Direct injection
Bore × Stroke	92 × 96 mm
Displacement	0.638 liter
Compression ratio	17.7
Rated output	8.1 kW @ 2400 rpm
Injection nozzle	4-hole nozzle
Nozzle opening pressure	19MPa

Table 2 Specifications of surfactants

	RHEODOL SP-L10	RHEODOL 440V	EMULGEN 103
Chemical name	Sorbitan monolaurate	Polyoxyethylene sorbitol tetraoleate	Polyoxyethylene lauryl ether
Appearance	Liquid	Liquid	Liquid
Freezing point (°C)	13-14	-	-
Acid value	4-7	10>	-
Saponification value	158-170	72-92	-
HLB	8.6	11.8	8.1

Table 3 Injection duration of each experiment [msec.] (* first injection/second injection)

Power [kW]	Speed [rpm]	LO	JO	JWE10%							
				JWE-23/0*		JWE-23/+3-large*		JWE-23/+3-small*		JWE-23/+6*	
3.0	2000	0.925	0.989	0.681	0.811	0.699	0.895	0.864	0.600	0.904	0.558
4.5	2000	1.017	0.1087	0.709	0.902	0.725	1.045	0.932	0.650	0.929	0.676
6.0	2000	1.149	1.196	0.710	1.122	0.726	1.140	0.964	0.657	0.989	0.695

Table 4 Properties of test fuels

Parameter	Light oil	JO	JWE10%
Density (kg/m^3) at 30 deg. C	821.45	895.4	913
Lower heating value (kJ/kg)	42490	39774	-
Viscosity (cSt) at 30 ^{o}C	19.1	44.7	48
Cetane number	45-55	40-45	-
Flash point (^{o}C)	50	240	-

Table 5 Main fatty acid composition of Jatropha oil

Fatty acid	% by weight	Systematic name	Structure	Formula
Oleic	40.5	Cis-9-Octadecenoic	18:1	$C_{18}H_{34}O_2$
Linoleic	35.9	Cis-9,cis-12-Octadecadienoic	18:2	$C_{18}H_{32}O_2$
Plamitic	6.8	Hexadecanoic	16:0	$C_{16}H_{32}O_2$
Vaccenic	1.0	(E)-Octadec-11-enoic	18:1	$C_{18}H_{34}O_2$
Linolenic	0.2	Cis-9,cis-12,cis-15-Octadecatrienoic	18:3	$C_{18}H_{30}O_2$
Arachidic	0.2	Eicosanoic	20:0	$C_{20}H_{40}O_2$
Palmitoleic	0.8	9-*cis*-Hexadecenoic	16:1	$C_{16}H_{30}O_2$